Multi-Objective Optimized OFDM Radar Waveform for Target Detection in Multipath Scenarios†

Satyabrata Sen, Gongguo Tang, and Arye Nehorai
Department of Electrical and Systems Engineering
Washington University in St. Louis
One Brookings Drive, St. Louis, MO 63130, USA
Email: {ssen3, gt2, nehorai}@ese.wustl.edu
Phone: 314-935-7520 Fax: 314-935-7500

***Abstract*—We propose a multi-objective optimization (MOO) technique to design an orthogonal frequency division multiplexing (OFDM) radar signal for detecting a moving target in the presence of multipath reflections. We employ an OFDM signal to increase the frequency diversity of the system. Moreover, the multipath propagation increase the spatial diversity by providing extra "looks" at the target. First, we develop a parametric measurement model by reformulating the target detection problem as a sparse estimation method. At a particular range cell, we exploit the sparsity of multiple paths and the knowledge of the environment to estimate along which path the target responses are received. Then, we formulate a constrained MOO algorithm, to optimally design the spectral parameters of the OFDM waveform, by simultaneously optimizing two objective functions: minimizing the upper bound on the estimation error to improve the efficiency of sparse-recovery and maximizing the squared Mahalanobis-distance to increase the performance of the underlying detection problem. We present numerical examples to demonstrate the performance improvement due to adaptive waveform design.**

I. Introduction

The problem of detection and tracking of targets in the presence of multipath, particularly in urban environments, are becoming increasingly relevant and challenging to radar technologies. In [1], [2], we have shown that the target detection capability can be significantly improved by exploiting multiple Doppler shifts corresponding to the projections of the target velocity on each of the multipath components. Furthermore, the multipath propagations increase the spatial diversity of the radar system by illuminating the target from different incident angles, and thus enabling target detection and tracking even beyond the line-of-sight (LOS) [3].

To resolve and exploit the multipath components it is generally common to use short pulse, multi-carrier wideband radar signals. We consider the orthogonal frequency division multiplexing (OFDM) signalling scheme [4], which is one of the ways to accomplish simultaneous use of several subcarriers. The use of OFDM signal mitigates the possible fading, resolves the multipath reflections, and provides additional frequency diversity as different scattering centers of a target resonate at different frequencies.

In this work, we consider a target detection problem in multipath scenarios from a different perspective (see also [5]). We observe that the radar receives the target information through an LOS and several reflected paths. Therefore, at first using the knowledge of the geometry, we can determine all the possible paths, be they LOS or reflected, and the associated target locations corresponding to a particular range cell. Then, considering the presence of a single target, we can apply any sparse signal recovery algorithms [6], [7], to single out along which path the target response is received. Thus, we transform the task of target detection into a sparse estimation problem.

First, in Section II, we develop a sparse measurement model that accounts for the target returns over all possible paths corresponding to a known range cell. For simplicity we consider only first-order reflections. In Section III, we present a sparsity-based recovery approach to decide about the presence of a target. We employ a collection of multiple small Dantzig selectors [7] that exploit more prior structures of the sparse vector. In Section IV, we propose to use a constrained multi-objective optimization (MOO) [8]-[10] to design the spectral parameters of the OFDM waveform. We consider two objective functions: minimize the upper bound on the estimation error to improve the efficiency of sparse-recovery and maximize the squared Mahalanobis-distance [11] to increase the performance of the underlying detection problem. We apply the well-known nondominated sorting genetic algorithm II (NSGA-II) [12] to obtain the Pareto-optimal solutions [8] of our MOO problem. We present numerical results in Section V to demonstrate the advantage of waveform design. Finally, concluding remarks are given in Section VI.

II. Problem Description and Modeling

Fig. 1 presents a schematic representation of the problem scenario. We consider a far-field point target in a multipath-rich environment, moving with a constant relative velocity $\boldsymbol{v}$ with respect to the radar. For simplicity we consider only the first-order specular reflections. We further assume that the radar has the complete knowledge of the environment that is under surveillance. This assumption implies that for

† This work was supported by the Department of Defense under the Air Force Office of Scientific Research MURI Grant FA9550-05-1-0443 and ONR Grant N000140810849.

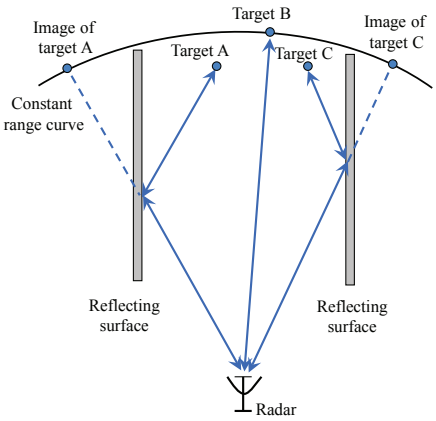

Fig. 1. A schematic representation of the multipath scenario.

a particular range cell (shown as the curved line in Fig. 1) the radar knows all the possible paths, be they LOS or reflected. Now, any target (e.g., Target B) or any image of a target (e.g., Target A or C) residing on the constant-range curved line has the same roundtrip delay and produces returns in the same range cell. Our goal here is to decide whether a target is present at the range cell under test.

We consider an OFDM signalling system with L active subcarriers, a bandwidth of B Hz, and pulse duration of T seconds. Let $\boldsymbol{a} = [a_0, a_1, \ldots, a_{L-1}]^T$ represent the complex weights transmitted over the L subcarriers, and satisfying $\sum_{l=0}^{L-1} |a_l|^2 = 1$. We incorporate information of the known range cell (denoted by the roundtrip delay τ) by substituting $t = \tau + nT_{\rm P}, n = 0, \ldots, N-1$, where $T_{\rm P}$ is the pulse repetition interval (PRI) and N is the number of temporal measurements within a given coherent processing interval (CPI). Then, corresponding to a specific range cell containing the target, the complex envelope of the received signal at the output of the l-th subchannel is

$$y_l(n) = a_l\, x_{lp}\, \widetilde{\phi}_l(n, p, \boldsymbol{v}) + e_l(n), \tag{1}$$

where x_{lp} is a complex quantity representing the scattering coefficient of the target along the l-th subchannel and p-th path; $\widetilde{\phi}_l(n, p, \boldsymbol{v}) \triangleq e^{-j2\pi f_l \tau}\, e^{j2\pi f_l \beta_p n T_{\rm P}}$; $\beta_p = 2\langle \boldsymbol{v}, \boldsymbol{u}_p \rangle / c$ is the relative Doppler shift along the p-th path; $\boldsymbol{u}_p$ represents the direction-of-arrival unit-vector of the p-th path; c is the speed of propagation; and $e_l(t)$ represents the clutter and measurement noise along the l-th subchannel.

Next, we discretize the possible signal paths and target velocities into P and V grid points, respectively. Restricting our operation to a narrow region of interest (e.g., an urban canyon where the range is much greater than the width) and a few class of targets that have comparable velocities (e.g., cars/trucks within a city environment), we can restrict the values of P and V to smaller numbers. Then, considering all possible combinations of $(p_i, \boldsymbol{v}_j), i = 1, 2, \ldots, P, j = 1, 2, \ldots, V$, we can rewrite (1) as

$$y_l(n) = a_l\, \widetilde{\boldsymbol{\phi}}_l(n)^T\, \boldsymbol{x}_l + e_l(n), \tag{2}$$

where $\widetilde{\boldsymbol{\phi}}_l(n) = \left[\widetilde{\phi}_l(n, p_1, \boldsymbol{v}_1), \ldots, \widetilde{\phi}_l(n, p_P, \boldsymbol{v}_V)\right]^T$; and $\boldsymbol{x}_l$ is a $PV \times 1$ sparse-vector, having only k_l non-zero entries corresponding to the true signal paths and target velocity.

Concatenating the measurements of all subchannels and temporal points we get

$$\boldsymbol{y} = \boldsymbol{\Phi}\, \boldsymbol{x} + \boldsymbol{e}, \tag{3}$$

where $\boldsymbol{y} = \left[\boldsymbol{y}(0)^T, \ldots, \boldsymbol{y}(N-1)^T\right]^T$ is an $LN \times 1$ vector with $\boldsymbol{y}(n) = [y_0(n), \ldots, y_{L-1}(n)]^T$; $\boldsymbol{\Phi} = \left[\left(\boldsymbol{A}\widetilde{\boldsymbol{\Phi}}(0)\right)^T \cdots \left(\boldsymbol{A}\widetilde{\boldsymbol{\Phi}}(N-1)\right)^T\right]^T$ is an $LN \times LPV$ matrix, containing all possible combinations of signal path and target velocity, with $\boldsymbol{A} = \mathrm{diag}(\boldsymbol{a})$ and $\widetilde{\boldsymbol{\Phi}}(n) = \mathrm{blkdiag}\left(\widetilde{\boldsymbol{\phi}}_0(n)^T, \ldots, \widetilde{\boldsymbol{\phi}}_{L-1}(n)^T\right)$; $\boldsymbol{x} = \left[\boldsymbol{x}_0^T, \ldots, \boldsymbol{x}_{L-1}^T\right]^T$ is an $LPV \times 1$ sparse-vector that has $k = \sum_{l=0}^{L-1} k_l$ non-zero entries; and $\boldsymbol{e} = \left[\boldsymbol{e}(0)^T, \ldots, \boldsymbol{e}(N-1)^T\right]^T$ is an $LN \times 1$ vector, comprising of clutter returns, noise, and interference, with $\boldsymbol{e}(n) = [e_0(n), \ldots, e_{L-1}(n)]^T$. We assume that $\boldsymbol{e}(n)$ is a temporally white complex Gaussian vector, distributed as $\boldsymbol{e} \sim \mathbb{C}\mathcal{N}_{LN}\,(\boldsymbol{0},\, \boldsymbol{I}_N \otimes \boldsymbol{\Sigma})$.

III. Sparse Recovery

The goal of the sparse recovery algorithm is to estimate the vector $\boldsymbol{x}$ from the noisy measurement $\boldsymbol{y}$ in (3) by exploiting the sparsity. However, from the discussion of the previous section we observe an additional structure in $\boldsymbol{x}$, described as follows:

$$\boldsymbol{x} = \left[\boldsymbol{x}_0^T, \boldsymbol{x}_1^T, \ldots, \boldsymbol{x}_{L-1}^T\right]^T, \tag{4}$$

where each $\boldsymbol{x}_l$, $l = 0, \ldots, L-1$, is sparse with sparsity level $k_l = \|\boldsymbol{x}_l\|_0$, and $k = \sum_{l=0}^{L-1} k_l$. Furthermore, the system matrix $\boldsymbol{\Phi}$ in (3) can also be expressed as

$$\boldsymbol{\Phi} = [\, \boldsymbol{\Phi}_0 \quad \boldsymbol{\Phi}_1 \quad \cdots \quad \boldsymbol{\Phi}_{L-1} \,], \tag{5}$$

where each block-matrix, of dimension $LN \times PV$, is orthogonal to any other block-matrix; i.e., $\boldsymbol{\Phi}_{l_1}^H \boldsymbol{\Phi}_{l_2} = \boldsymbol{0}$ for $l_1 \neq l_2$. Note the difference in notation between $\boldsymbol{\Phi}_l$ (which is a columnwise block-matrix) and $\widetilde{\boldsymbol{\Phi}}(n)$ (which is a rowwise block-matrix).

To exploit this additional structure in the sparse-recovery algorithm, we propose a reconstruction algorithm that solves L small Dantzig selectors (DS) [7] to provide an estimate of $\boldsymbol{x}$ as the solution to the following ℓ_1-regularization problems:

$$\min_{\boldsymbol{z}_l \in \mathbb{C}^{PV}} \|\boldsymbol{z}_l\|_1 \quad \text{subject to} \quad \left\| \boldsymbol{\Phi}_l^H \left(\boldsymbol{y} - \boldsymbol{\Phi}_l \boldsymbol{z}_l\right) \right\|_\infty \leq \lambda_l \cdot \sigma, \tag{6}$$

where $\lambda_l = \sqrt{2\,\log(PV)}$ is a control parameter and $\sigma = \sqrt{\mathrm{tr}\Sigma / L}$.

To analyze the reconstruction performance we consider a new, easily computable measure ℓ_1-constrained minimal singular value (ℓ_1-CMSV) of the measurement matrix [13]. Accordingly, the performance of our decomposed DS in (6) is given by the following theorem:

Theorem 1: Suppose $\boldsymbol{x} \in \mathbb{C}^{LPV}$ is a k-sparse vector having an additional structure as presented in (4), with each

$\boldsymbol{x}_l \in \mathbb{C}^{PV}$ being a k_l-sparse vector, and (3) is the measurement model. Choose $\lambda_l = \sqrt{2\,\log(PV)}$ in (6). Then, with high probability, $\widehat{\boldsymbol{x}}$ satisfies

$$\|\widehat{\boldsymbol{x}} - \boldsymbol{x}\|_2 \;\leq\; 4\,\sqrt{\sum_{l=0}^{L-1} \frac{\lambda_l^2\, k_l\, \sigma^2}{\rho_{4k_l}^4(\boldsymbol{\Phi}_l)}}\,, \tag{7}$$

where the concentrated solution $\widehat{\boldsymbol{x}} = \left[\widehat{\boldsymbol{x}}_0^T, \ldots, \widehat{\boldsymbol{x}}_{L-1}^T\right]^T$ is obtained by using the individual solutions, $\widehat{\boldsymbol{x}}_l$, of (6). More specifically, if $\lambda_l = \sqrt{2\,(1+q)\,\log(PV)}$ for each $q \geq 0$ is used in (6), the bound holds with probability greater than $1 - L\left(\sqrt{\pi\,(1+q)\,\log(PV)}\cdot(PV)^q\right)^{-1}$.

Proof: See [5]. ∎

IV. Adaptive Waveform Design

From the discussion of the previous section it follows that we can adaptively design the signal parameters, a_l, to minimize the upper bound on the estimation error. Note here that the upper bound on the sparse-estimation error depends solely on the properties of $\boldsymbol{\Phi}$ and noise level σ^2. However, to achieve better performance it is also essential that the signal parameters are adaptive to the operational scenario involving dynamic target states and non-stationary environmental conditions. Hence, in addition to minimizing the upper bound on the estimation error, we propose maximizing another utility function based on the squared Mahalanobis-distance, which depends on the target and noise parameters ($\boldsymbol{x}$ and $\boldsymbol{\Sigma}$). In the following, we first describe these two single-objective optimization problems and their respective solutions. Then, we discuss the multi-objective optimization method.

A. Minimizing the Error Bound

From (5), we first notice that each $\boldsymbol{\Phi}_l$ can be written as $\boldsymbol{\Phi}_l = a_l\widetilde{\boldsymbol{\Phi}}_l$, and therefore we have $\rho_{4k_l}^4(\boldsymbol{\Phi}_l) = a_l^4\,\rho_{4k_l}^4(\widetilde{\boldsymbol{\Phi}}_l)$. Then, to minimize the upper bound on the sparse-estimation error, we construct an optimization problem as

$$\boldsymbol{a}^{(1)} = \arg\min_{\boldsymbol{a}\,\in\,\mathbb{C}^L} \sum_{l=0}^{L-1} \frac{\lambda_l^2\, k_l\, \sigma^2}{a_l^4\,\rho_{4k_l}^4(\widetilde{\boldsymbol{\Phi}}_l)} \quad \text{subject to } \boldsymbol{a}^H\boldsymbol{a} = 1. \tag{8}$$

Using the Lagrange-multiplier approach, we can easily obtain the solution of (8) as

$$a_l^{(1)} = \sqrt{\frac{(2\alpha_l)^{1/3}}{\sum_{l=0}^{L-1}\,(2\alpha_l)^{1/3}}}, \quad \text{for } \; l = 0, 1, \ldots, L-1, \tag{9}$$

where $\alpha_l = \frac{\lambda_l^2\, k_l\, \sigma^2}{\rho_{4k_l}^4(\widetilde{\boldsymbol{\Phi}}_l)}$. However, the computation of $\rho_{4k_l}(\widetilde{\boldsymbol{\Phi}}_l)$ is difficult with the complex variables. Therefore, we use a computable lower bound on $\rho_{4k_l}(\widetilde{\boldsymbol{\Phi}}_l)$, defined as

$$\rho_{8k_l}(\widetilde{\boldsymbol{\Psi}}) \;\leq\; \rho_{4k_l}(\widetilde{\boldsymbol{\Phi}}_l), \tag{10}$$

where

$$\begin{aligned} \widetilde{\boldsymbol{\Psi}}^T\,\widetilde{\boldsymbol{\Psi}} \;&=\; \begin{bmatrix} \boldsymbol{\Psi}_1^T\,\boldsymbol{\Psi}_1 + \boldsymbol{\Psi}_2^T\,\boldsymbol{\Psi}_2 & \boldsymbol{0} \\ \boldsymbol{0} & \boldsymbol{\Psi}_1^T\,\boldsymbol{\Psi}_1 + \boldsymbol{\Psi}_2^T\,\boldsymbol{\Psi}_2 \end{bmatrix}, \\ \boldsymbol{\Psi}_1 \;&=\; \mathrm{Re}\,\widetilde{\boldsymbol{\Phi}}_l, \quad \boldsymbol{\Psi}_2 \;=\; \mathrm{Im}\,\widetilde{\boldsymbol{\Phi}}_l. \end{aligned} \tag{11}$$

See [5] for the details of (10). Then, similar to (9), we can obtain the optimal OFDM weights as

$$a_l^{(1)} = \sqrt{\frac{(2\widetilde{\alpha}_l)^{1/3}}{\sum_{l=0}^{L-1}\,(2\widetilde{\alpha}_l)^{1/3}}}, \quad \text{for } \; l = 0, 1, \ldots, L-1, \tag{12}$$

where $\widetilde{\alpha}_l = \frac{\lambda_l^2\, k_l\, \sigma^2}{\rho_{8k_l}^4(\widetilde{\boldsymbol{\Psi}})}$.

B. Maximizing the Mahalanobis-Distance

To decide whether a target is present or not in the range cell under test, the standard procedure is to construct a decision problem to choose between two possible hypotheses: the null hypothesis $\mathcal{H}_0$ (target-free hypothesis) or the alternate hypothesis $\mathcal{H}_1$ (target-present hypothesis). The problem can be expressed as

$$\begin{cases} \mathcal{H}_0: & \boldsymbol{y} = \boldsymbol{e} \\ \mathcal{H}_1: & \boldsymbol{y} = \boldsymbol{\Phi}\,\boldsymbol{x} + \boldsymbol{e} \end{cases}. \tag{13}$$

Hence, the measurement $\boldsymbol{y}$ is distributed as either $\mathbb{CN}_{LN}\,(\boldsymbol{0},\, \boldsymbol{I}_N \otimes \boldsymbol{\Sigma})$ or $\mathbb{CN}_{LN}\,(\boldsymbol{\Phi}\boldsymbol{x},\, \boldsymbol{I}_N \otimes \boldsymbol{\Sigma})$. To distinguish between these two distributions, one standard measure is the squared Mahalanobis-distance [11], defined as

$$d^2 \;\;=\;\; \boldsymbol{x}^H\,\boldsymbol{\Phi}^H\,\left(\boldsymbol{I}_N \otimes \boldsymbol{\Sigma}\right)^{-1}\,\boldsymbol{\Phi}\,\boldsymbol{x}. \tag{14}$$

Then, to maximize the detection performance, we can formulate an optimization problem as

$$\boldsymbol{a}^{(2)} = \arg\max_{\boldsymbol{a}\,\in\,\mathbb{C}^L} \left[\boldsymbol{x}^H\,\boldsymbol{\Phi}^H\,\left(\boldsymbol{I}_N \otimes \boldsymbol{\Sigma}\right)^{-1}\,\boldsymbol{\Phi}\,\boldsymbol{x}\right], \tag{15}$$

subject to $\boldsymbol{a}^H\boldsymbol{a} = 1$. After some algebraic manipulations (see [5] for details) we can rewrite this problem as

$$\boldsymbol{a}^{(2)} = \arg\max_{\boldsymbol{a}\,\in\,\mathbb{C}^L} \; \boldsymbol{a}^H\,\boldsymbol{Q}\,\boldsymbol{a}, \quad \text{subject to } \boldsymbol{a}^H\boldsymbol{a} = 1, \tag{16}$$

where $\boldsymbol{Q} = \sum_{n=0}^{N-1}\left(\widetilde{\boldsymbol{\Phi}}(n)\,\boldsymbol{x}\,\boldsymbol{x}^H\,\widetilde{\boldsymbol{\Phi}}(n)^H\right)^T \odot \boldsymbol{\Sigma}^{-1}$. Hence, the optimization problem reduces to a simple eigenvalue-eigenvector problem, and the solution of (16) is the eigenvector corresponding to the largest eigenvalue of $\boldsymbol{Q}$.

C. Multi-Objective Optimization

From the discussions of previous subsections we notice that if the solution of (12) is used one would achieve an efficient sparse-estimation result. Alternatively, solving (16) we might get improved performance of the underlying detection problem. Hence, based on these arguments, we devise a constrained MOO problem to design the spectral parameters of the OFDM waveform such that the upper bound on the sparse-estimation error is minimized and the squared Mahalanobis-distance of the detection problem is simultaneously maximized. Mathematically, this is represented as

$$\boldsymbol{a}_{\mathrm{opt}} = \left\{ \begin{array}{l} \arg\min_{\boldsymbol{a}} \;\; \sum_{l=0}^{L-1} \frac{\lambda_l^2\, k_l\, \sigma^2}{a_l^4\,\rho_{8k_l}^4(\widetilde{\boldsymbol{\Psi}})} \\ \arg\max_{\boldsymbol{a}} \;\; \boldsymbol{a}^H\,\boldsymbol{Q}\,\boldsymbol{a} \end{array} \right\} \text{subject to } \boldsymbol{a}^H\boldsymbol{a} = 1. \tag{17}$$

We employ the standard nondominated sorting genetic algorithm II (NSGA-II) [12] to solve our MOO problem, constraining the solutions to satisfy $\boldsymbol{a}^H\boldsymbol{a} = 1$. The use of NSGA-II

provides us with multiple Pareto-optimal solutions in a single run.

V. Numerical Results

In this section, we present the results of several numerical examples to demonstrate the performance improvement due to the adaptive OFDM waveform design technique. For simplicity we considered a 2D scenario. Throughout a given CPI the target remained within a particular range cell that was at a distance of 3 km from the radar (positioned at the origin). The target was 13.5 m east from the center line, moving with velocity $\boldsymbol{v} = (35/\sqrt{2})\,(\hat{\imath} + \hat{\jmath})$ m/s. There were two different paths between the target and radar: one direct and one reflected, subtending angles of 0.26° and 0.51°, respectively, with respect to the radar. We considered an OFDM radar operating with the following specifications: carrier frequency $f_{\rm c} = 1$ GHz; bandwidth $B = 100$ MHz; number of OFDM subcarriers $L = 3$; subcarrier spacing of $\Delta f = B/(L+1) = 25$ MHz; pulse width $T = 1/\Delta f = 40$ ns; pulse repetition interval $T_{\rm P} = 4$ ms; number of coherent pulses $N = 20$; and all the transmit OFDM weights were equal, i.e., $a_l = 1/\sqrt{L}\ \forall\, l$.

To apply a sparse estimation approach, we partitioned the signal paths and target velocities into $P = 5$ and $V = 3$ uniform grid points. We considered signal paths that subtended angles of $\{-0.5^\circ, -0.25^\circ, 0^\circ, 0.25^\circ, 0.5^\circ\}$ with respect to the radar and target velocities of $\{25, 35, 45\}$ m/s. Hence, we had $k_l = 2\ \forall\, l$ and $k = 6$. We generated the noise samples from a $\mathbb{CN}(0,1)$ distribution, and then scaled the samples to satisfy the required target to clutter-plus-noise ratio ($\mathrm{TCNR} = \left[\boldsymbol{x}^H \boldsymbol{x}\right] / \left[N\, L\, \sigma_0^2\right]$). Here we kept the clutter-plus-noise power to be the same across all the subcarriers by considering $\boldsymbol{\Sigma} = \sigma_0^2\, \boldsymbol{I}_L$. The scattering coefficients, $\boldsymbol{x}$, were varied to simulate three different targets in our simulations. Target 1 had equal scattering responses across all the subcarriers; i.e., $x_{l,\rm d}^{(1)} = [1,1,1]^T$ and $x_{l,\rm r}^{(1)} = [0.5, 0.5, 0.5]^T$ were the scattering coefficients of Target 1 along the direct and reflected paths, respectively. For Target 2 and Target 3 we considered varying responses over different subcarriers; i.e., $x_{l,\rm d}^{(2)} = [4,1,2]^T$, $x_{l,\rm r}^{(2)} = [2, 0.5, 2]^T$, and $x_{l,\rm d}^{(3)} = [1,10,1]^T$, $x_{l,\rm r}^{(3)} = [0.5, 5, 0.5]^T$, respectively.

To solve the MOO problem (17), we employed the NSGA-II with the following parameters: population size $= 500$, number of generations $= 50$, crossover probability $= 0.9$, and mutation probability $= 0.1$. We applied the constraint $\boldsymbol{a}^H \boldsymbol{a} = 1$ in a relaxed way by ensuring that the solutions satisfy $0.999 \le \boldsymbol{a}^H \boldsymbol{a} \le 1.001$. We plotted the results of the optimal solutions and corresponding values of the two objective functions (at two different generations) in Figs. 2 and 3 for Targets 1 and 2, respectively.

To investigate on the relationship between the distributions of energy of the optimal waveform, $\boldsymbol{a}_{\rm opt}$, and target response, $\boldsymbol{x}$, along different subcarriers, we took the average over the whole population of 500 solutions and found $\boldsymbol{a}_{\rm opt,avg} = [0.61, 0.39, 0.68]^T$ for Target 1 and $\boldsymbol{a}_{\rm opt,avg} = [0.88, 0.20, 0.36]^T$ for Target 2. Though it is not clear for

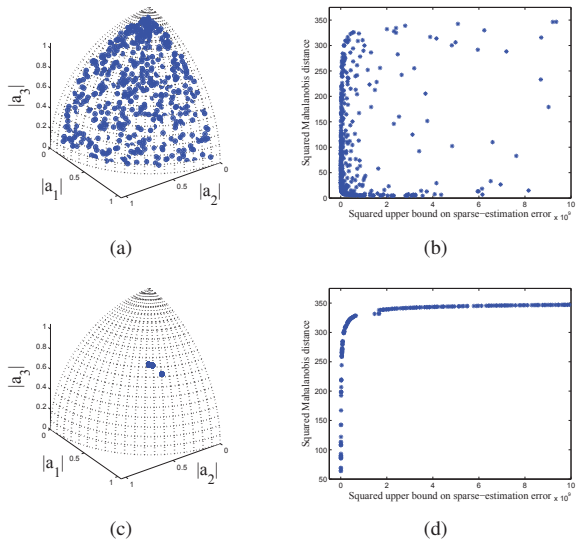

Fig. 2. Results of the NSGA-II for Target 1: (a), (b) optimal solutions and values of the objective functions at 0-th generation; (c), (d) optimal solutions and values of the objective functions at 50-th generation.

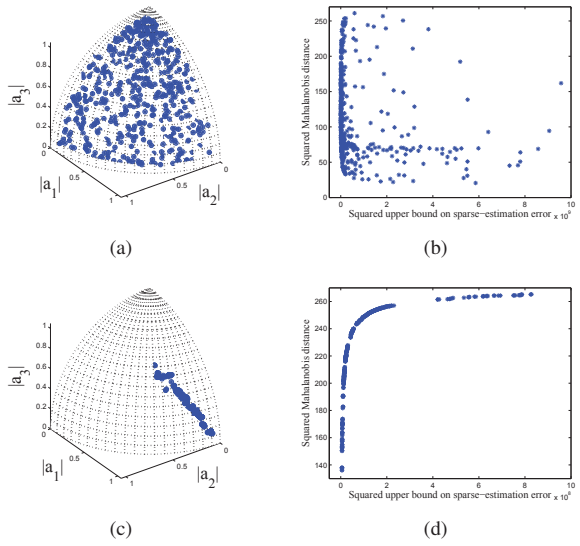

Fig. 3. Results of the NSGA-II for Target 2: (a), (b) optimal solutions and values of the objective functions at 0-th generation; (c), (d) optimal solutions and values of the objective functions at 50-th generation.

Target 1, from the results of Target 2 we observed that the averaged distributions of energy of the optimal waveform across different subcarriers are in proportions to the distributions of target energy. As further confirmation, we ran the NSGA-II for Target 3 as well. Fig. 4 depicts the optimal solutions and corresponding values of the objective functions at the end of the 50-th generation. In this case the average over all 500 solutions was $\boldsymbol{a}_{\rm opt,avg} = [0.13, 0.96, 0.15]^T$. Hence, in general we can conclude that the solution of the MOO distributes the energy of the optimal waveform across different subcarriers in

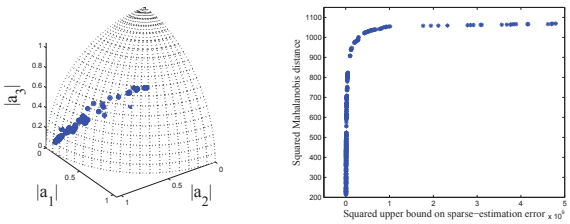

(a) (b)

Fig. 4. Results of the NSGA-II for Target 3: (a), (b) optimal solutions and values of the objective functions at 50-th generation.

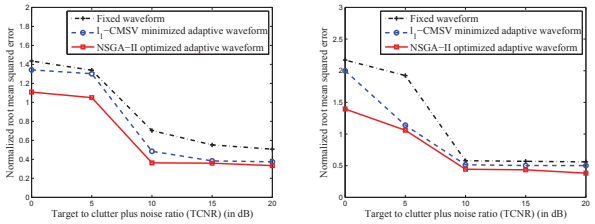

(a) (b)

Fig. 5. Comparison of performances due to the fixed and adaptive waveforms to detect (a) Target 2 and (b) Target 3 in terms of normalized RMSE vs. target to clutter-plus-noise ratio.

proportion to the distribution of the target energy; i.e., it puts more signal energy into that particular subcarrier in which the target response is stronger.

We took one of the solutions from the Pareto front after the 50-th generation (e.g., $\boldsymbol{a}_{\rm opt} = [0.98, 0.11, 0.17]^T$ for Target 2 and $\boldsymbol{a}_{\rm opt} = [0.22, 0.93, 0.29]^T$ for Target 1) and evaluated the performance characteristics of our system. The results are shown in Fig. 5 for Targets 2 and 3. We observed that due to its dependance on the target parameters the NSGA-II optimized waveform, $\boldsymbol{a}_{\rm opt}$, performed better than both the ℓ_1-CMSV–based adaptive waveform, $\boldsymbol{a}^{(1)}$, and a fixed waveform having $a_l = 1/\sqrt{L}\ \forall l$.

Minimizing the upper bound on the sparse-estimation error, i.e., as a solution of (12), yielded $\boldsymbol{a}^{(1)} = [0.54, 0.16, 0.83]$. This solution depends only on the properties of the system matrix $\boldsymbol{\Phi}$. It implies that we can expect improved performance due to the use of this $\boldsymbol{a}^{(1)}$ irrespective of the target and noise parameters, which is evident from Fig. 5 for Targets 2 and 3.

In (16), the matrix $\boldsymbol{Q}$ became diagonal due to the choice of $\boldsymbol{\Sigma} = \sigma_0^2 \boldsymbol{I}_L$. Therefore, the eigenvector corresponding to the largest eigenvalue had only one entry equal to 1 with all others 0. For example, in the case of Target 2, which had stronger reflection along the first subcarrier, the solution of (16) was $\boldsymbol{a}^{(2)} = [1, 0, 0]^T$; whereas for Target 3 we found the optimal solution to be $\boldsymbol{a}^{(2)} = [0, 1, 0]^T$. Hence, we concluded that the maximization of Mahalanobis distance effectively results in a single-carrier waveform that could not provide any frequency diversity. Therefore, we did not analyze the performance of our system with this type of adaptive waveform.

VI. Conclusions

In this paper, we proposed a multi-objective optimization (MOO) technique to design the spectral parameters of an orthogonal frequency division multiplexing (OFDM) radar signal for detecting a moving target in the presence of multipath reflections. We first developed a parametric measurement model by reformulating the target detection problem as a sparse estimation method. Using the knowledge of the geometry and all possible paths through which the target information are received, we applied a sparse signal recovery algorithm to determine the true path of the target returns. We also analytically evaluated the performance characteristics using the ℓ_1-constrained minimal singular value of the measurement matrix. Then, we proposed to design the spectral parameters of the OFDM waveform using a constrained MOO algorithm with two simultaneous objectives: minimizing the upper bound on the estimation error and maximizing the squared Mahalanobis-distance. We presented numerical examples showing the performance improvement that could be obtained due to such adaptive waveform design. In our future work, we will incorporate other waveform design criteria, e.g., ambiguity function, into the MOO algorithm. We will also validate the proposed technique with real data.

References

[1] S. Sen, M. Hurtado, and A. Nehorai, "Adaptive OFDM radar for detecting a moving target in urban scenarios," in *Proc. 4th Int. Waveform Diversity & Design (WDD) Conf.*, Orlando, FL, Feb. 8–13, 2009, pp. 268–272.

[2] S. Sen and A. Nehorai, "Adaptive OFDM radar for target detection in multipath scenarios," *IEEE Trans. Signal Process.*, to appear.

[3] J. L. Krolik, J. Farrell, and A. Steinhardt, "Exploiting multipath propagation for GMTI in urban environments," in *IEEE Conf. on Radar*, 24–27, 2006, pp. 65–68.

[4] T. May and H. Rohling, "Orthogonal frequency division multiplexing," in *Wideband Wireless Digital Communications*, A. F. Molisch, Ed. Upper Saddle River, NJ: Prentice Hall PTR, 2001, ch. 17-25.

[5] S. Sen, G. Tang, and A. Nehorai, "Multi-objective optimization-based OFDM radar waveform design for target detection," *IEEE Trans. Signal Process.*, submitted.

[6] S. S. Chen, D. L. Donoho, and M. A. Saunders, "Atomic decomposition by basis pursuit," *SIAM Jour. on Scientific Computing*, vol. 20, no. 1, pp. 33–61, Aug. 1998.

[7] E. Candès and T. Tao, "The Dantzig selector: Statistical estimation when p is much larger than n," *The Annals of Statistics*, vol. 35, no. 6, pp. 2313–2351, 2007.

[8] K. Deb, *Multi-Objective Optimization Using Evolutionary Algorithms*, 1st ed. John Wiley & Sons, Jun. 2001.

[9] C. A. C. Coello, G. B. Lamont, and D. A. V. Veldhuizen, *Evolutionary Algorithms for Solving Multi-Objective Problems*, 2nd ed. New York, NY: Springer, 2007.

[10] R. T. Marler and J. S. Arora, "Survey of multi-objective optimization methods for engineering," *Structural and multidisciplinary optimization*, vol. 26, no. 6, pp. 369–395, Mar. 2004.

[11] T. W. Anderson, *An Introduction to Multivariate Statistical Analysis*, 3rd ed. Hoboken, NJ: John Wiley & Sons, Inc., 2003.

[12] K. Deb, A. Pratap, S. Agarwal, and T. Meyarivan, "A fast and elitist multiobjective genetic algorithm: NSGA-II," *IEEE Trans on Evolutionary Computation*, vol. 6, no. 2, pp. 182–197, Apr. 2002.

[13] G. Tang and A. Nehorai, "The ℓ_1-constrained minimal singular value: A computable quantification of the stability of sparse signal reconstruction," *IEEE Trans. Inf. Theory*, Apr. 2010, submitted. [Online]. Available: http://arxiv.org/abs/1004.4222v1